

# Oxidation of C4-hydroxyphenyl 1,4-dihydropyridines in dimethylsulfoxide and its reactivity towards alkylperoxyl radicals in aqueous medium

Luis J. Núñez-Vergara,<sup>a,\*</sup> R. Salazar,<sup>a</sup> C. Camargo,<sup>b</sup> J. Carbajo,<sup>d</sup> B. Conde,<sup>d</sup>  
P. A. Navarrete-Encina<sup>c</sup> and J. A. Squella<sup>a</sup>

<sup>a</sup>Laboratory of Bioelectrochemistry, Faculty of Chemical and Pharmaceutical Sciences,  
University of Chile, PO Box 233, Santiago, Chile

<sup>b</sup>Laboratory of Antidoping, Faculty of Chemical and Pharmaceutical Sciences, University of Chile, PO Box 233, Santiago, Chile

<sup>c</sup>Laboratory of Organic Synthesis and Molecular Modeling, Faculty of Chemical and Pharmaceutical Sciences,  
University of Chile, PO Box 233, Santiago, Chile

<sup>d</sup>Facultad de Ciencias Experimentales, Universidad de Huelva, Huelva, Spain

---

**Abstract**—This work reports the electrochemical oxidation of three newly synthesized C4-hydroxyphenyl-substituted 1,4-dihydropyridine derivatives in dimethylsulfoxide. The reactivity of the compounds with ABAP-derived alkylperoxyl radicals in aqueous buffer pH 7.4, was also studied.

The oxidation mechanism involves the formation of the unstable dihydropyridyl radical, which was confirmed by controlled-potential electrolysis (CPE) and ESR experiments. The final product of the CPE, that is, pyridine derivative, was identified by GC–MS technique for the three derivatives.

A direct reactivity of the synthesized compounds toward ABAP-derived alkylperoxyl radicals was found. The pyridine derivative was identified by GC–MS as the final product of the reaction. Results reveal that this type of 1,4-DHPs significantly reacts with the radicals, even compared with commercial 1,4-DHP drugs with a well-known antioxidant ability.

---

## 1. Introduction

4-Aryl-1,4-dihydropyridines (1,4-DHPs) are the most studied class of organic calcium channel modulators and, since their introduction into clinical medicine in 1975, have become almost indispensable for the treatment of cardiovascular diseases such as hypertension, cardiac arrhythmias, or angina.<sup>1–3</sup> Substantial research has been devoted to the chemistry and biology of the 1,4-DHP derivatives because of their applications in other hot areas such as synthesis of substituted pyridines<sup>2,4</sup>; serving as effective redox catalysts under mild conditions,<sup>5</sup> modeling the NAD(P)H coenzymes to study its oxidation mechanism in living system,<sup>6</sup> and

emerging as a common nucleus to numerous bioactive compounds.<sup>7,8</sup>

The oxidation of 1,4-dihydropyridines and analogs to the corresponding pyridines is of interest because of its relevance to the biological NADH redox processes as well as to the metabolic studies pertaining to 1,4-DHPs.<sup>9,10</sup> The electrochemical oxidation of 1,4-DHPs has extensively been reported in different electrolytic media by other.<sup>11–17</sup> and us.<sup>18–22</sup>

There are several in vitro findings that DHP calcium antagonists possess antioxidant properties, mainly during the development of atherosclerosis and some cardiovascular oxidative processes.<sup>23–28</sup> For some years our laboratory has been interested in the synthesis of new 1,4-DHPs in order to achieve derivatives with additional properties, mostly as antioxidants. Then, considering the relevance of its oxidation process on

---

*Keywords:* Voltammetry; ESR; GC–MS; Glassy carbon electrode; C4-hydroxyphenyl; 1,4-Dihydropyridines; Oxidation; Alkylperoxyl radicals.

\* Corresponding author. E-mail: lnunezv@ciq.uchile.cl

the biological activity; in the present paper we report a comparative study on the electrochemical oxidation in dimethylsulfoxide of new C4- hydroxyphenyl substituted 1,4-dihydropyridines with the corresponding C4- phenyl 1,4-dihydropyridine. The reactivity of the derivatives with ABAP-derived alkylperoxyl radicals was also studied.

## 2. Results and discussion

The main goal of this work was the study of both the electrochemical oxidation in DMSO and the reactivity with alkylperoxyl ABAP-derived radicals of three synthesized 1,4-dihydropyridines. Also, we have conducted a number of additional experiments to support the proposed mechanisms on the electrochemical oxidation and its reactivity with free radicals.

### 2.1. Voltammetry

In the aprotic medium, we have compared the anodic oxidation of the phenylhydroxyl-substituted compounds [4-(3-hydroxyphenyl)-DHP and 4-(4-hydroxyphenyl)-DHP] with the non-hydroxylated compound (4-phenyl-DHP). Tested derivatives exhibited a single anodic signal with the following oxidation peak potential values: 4-(4-hydroxyphenyl)-DHP ( $E_p = 1040$  mV), 4-(3-hydroxyphenyl)-DHP ( $E_p = 1048$  mV, Fig. 1a), and 4-phenyl-DHP ( $E_p = 1064$  mV, Fig. 2a). As can be seen from these values, there are not significant differences between the compounds.

Cyclic voltammetric studies were performed at different sweep rates (0.1–5.0 V/s) with the three compounds revealing a single irreversible anodic peak. In all the cases,  $\log i_p$  versus  $\log v$  plots exhibited slopes close to 0.5, thus indicating that the current is diffusion-controlled. Furthermore, the peak potential values ( $E_p$ ) were dependent on the sweep rates, indicating the irreversible character of the process.

The behavior of the limiting current was analyzed by using dynamic voltammetry on a glassy carbon rotating disk electrode. Compounds show a single wave with no indication of other oxidation waves. Limiting current versus the square root of the rotating rate were plotted to obtain the respective diffusion coefficients. These plots were linear (result not shown) according to the Levich equation.<sup>29</sup> From the slopes of these lines, the following diffusion coefficient values were obtained: 4-phenyl-DHP,  $2.81 \times 10^{-6}$  ( $\text{cm}^2 \text{s}^{-1}$ ); 4-(3-hydroxyphenyl)-DHP,  $3.10 \times 10^{-6}$  ( $\text{cm}^2 \text{s}^{-1}$ ), and 4-(4-hydroxyphenyl)-DHP,  $2.40 \times 10^{-6}$  ( $\text{cm}^2 \text{s}^{-1}$ ). In consequence, no significant differences in these values are found.

**2.1.1. Coulometric analysis.** In order to understand the mechanism of oxidation in greater detail and to determine the number of electrons involved in the oxidation process, coulometric studies were carried out in aprotic media. Solutions containing accurately weighed amount of the 1,4-dihydropyridine derivatives with TBAHFP

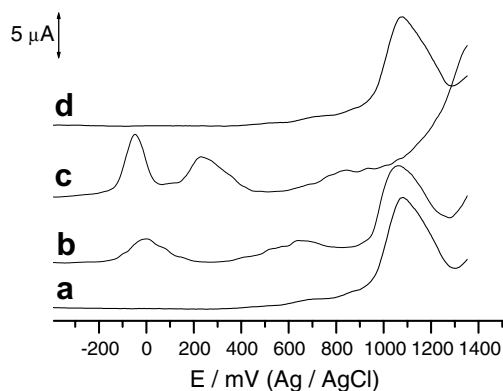


**Figure 1.** DP voltammograms of: (a) 1 mM 4-(3-hydroxyphenyl)-DHP solution in dimethylsulfoxide. (b) Solution (A) +2.5 mM TBA-OH. (c) Solution (B) +7.0 mM TBA-OH. (d) Solution (C) +7.0 mM  $\text{HClO}_4$ .

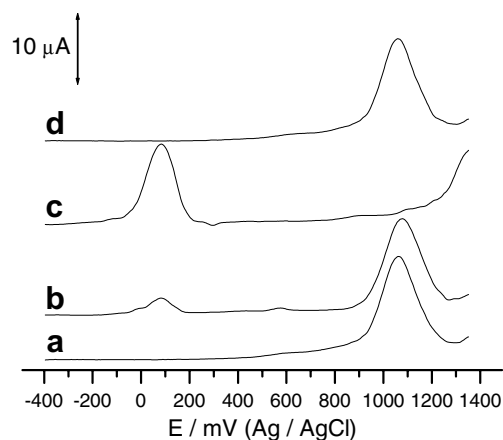


**Figure 2.** DP voltammograms of: (a) 1 mM 4-phenyl-DHP solution in dimethylsulfoxide. (b) Solution (A) +1.0 mM TBA-OH. (c) Solution (B) +2.5 mM. (d) Solution (C) +2.5 mM  $\text{HClO}_4$ .

were subjected to electrolysis at constant potential. The applied potential was +1180 mV for all the DHPs. Results show an average value for the electron transferred of  $2.10 \pm 0.15$  for the DHPs. These values are in accord with a two-electron oxidation mechanism for the oxidation of the DHP derivatives.

### 2.2. Influence of acid–base equilibrium on the electrochemical oxidation of the 1,4-dihydropyridine derivatives

For these studies we used electrochemical techniques (DPV and CV) and UV–visible spectroscopy. In Figure 2a, the DP voltammogram corresponding to the oxidation of 4-phenyl-DHP derivative exhibiting a peak at 1064 mV is shown. Figure 2b shows the effect of the addition of a 1.0 mM solution of tetrabutylammonium hydroxide (TBA-OH) on the oxidation of 4-phenyl-DHP. The intensity of the main signal decreased and in parallel the appearance of a new signal at approximately 108 mV is evidenced. The addition of 2.5 mM TBA-OH (Fig. 2c) produced a significant increase in the intensity of the signal at 108 mV parallel with the disappearance of the signal at 1064 mV. Finally, the addition of a 2.5 mM alcoholic  $\text{HClO}_4$  solution

(Fig. 2d) completely reversed the above-described effects, that is, the original signal at 1064 mV is recovered with no indication of the signal at 108 mV. On the other hand, if an  $\text{HClO}_4$  solution is first added to the original solution of 1,4-dihydropyridine, no changes are evidenced. These summarized effects can be explained by changes in the acid–base equilibrium of the secondary nitrogen of the 1-position. Thus, the main oxidation signal at 1064 mV corresponds to the oxidation of the unionized  $-\text{NH}$  group, in contrast the signal at 108 mV is the oxidation of ionized group, the anion ( $\text{R}-\text{N}^-$ ).

These types of experiments were extended for the hydroxyphenyl-substituted compounds (3-OH- and 4-(4-hydroxyphenyl)-DHPs). In Figure 1, the effect of the addition of TBA-OH is illustrated for the 4-(3-hydroxyphenyl)-DHP compound. The Figure 1a shows a typical DP voltammogram corresponding to 4-(3-hydroxyphenyl)-DHP derivative in which the single oxidation peak at 1048 mV is displayed. The addition of a 3.0 mM solution of TBA-OH (Fig. 1b) produced a decrease in the intensity of the original signal at 1048 mV, parallel with the appearance of a new oxidation signal with a peak potential value of  $-48$  mV. However, the addition of a 7.0 mM solution of TBA-OH (Fig. 1c) produced an increase in the signal intensity at  $-48$  mV, parallel with the appearance of a new signal at 244 mV and the disappearance of the original signal at 1048 mV. The addition of 7.0 mM  $\text{HClO}_4$  solution completely reversed the effects of the TBA-OH, that is, the original oxidation signal at 1048 mV appeared. In the case of the 4-(4-hydroxyphenyl)-DHP derivative, the addition of a 3.0 mM solution of TBA-OH produced a decrease in the intensity of the original signal at 1040 mV, parallel with the appearance of a new oxidation signal with a peak potential value of  $-92$  mV. On the other hand, the addition of a 7.0 mM solution of TBA-OH produced an increase in the signal intensity at  $-92$  mV, parallel with the appearance of a new signal at 156 mV and the complete disappearance of the original signal at 1040 mV. Likewise of 4-(3-hydroxyphenyl)-DHP derivative, the addition of 7.0 mM  $\text{HClO}_4$  solution completely reversed the effects of the TBA-OH, that is, the original oxidation signal at 1040 mV again appeared.

These above-described results could be explained by changes in the acid–base equilibrium involving the N–H and O–H groups. The signal at 244 mV could be assigned to the oxidation of the phenolate anion ( $\text{R}-\text{O}^-$ ) and the second one at  $-48$  mV would correspond to the oxidation of the anion ( $\text{R}-\text{N}^-$ ). This explanation is consistent with the finding that the addition of  $\text{HClO}_4$  to the 1,4-dihydropyridine solution (Fig. 1d) completely reversed the coexistence of several oxidation processes, that is, only one oxidation peak is evidenced ( $E_p = 1048$  mV).

Some additional experiments were conducted in order to deepen in the effects of acid–base equilibrium on the oxidation process of the compounds. In this perspective, the oxidation of a phenol solution under the same experimental conditions as the hydroxyphenyl-substituted 1,4-dihydropyridines was studied. Figure 3a shows the oxidation of a 1 mM phenol solution in DMSO, which

exhibited a potential value of 1208 mV. In Figure 3b, the effect of 2.0 mM TBA-OH solution on the oxidation of phenol is displayed. As can be seen, the intensity of the original oxidation signal at 1208 mV decreased concomitantly with the appearance of a new oxidation signal at 208 mV. This latter signal corresponds to the oxidation of the phenolate anion ( $\text{R}-\text{O}^-$ ). A second addition of 4.0 mM TBA-OH (Fig. 3c) produced a significant increase in the intensity of the signal at 208 mV with the disappearance of the original signal at 1208 mV.

From the above-described results it appears that the eventual oxidation of the hydroxyphenyl moiety in the electrolytic medium would occur at potential nearby to the supporting electrolyte discharge. In fact, the electrochemical studies (dpv, cv, coulometric analysis, RDE technique) conducted to characterize the oxidation process of the synthesized DHPs correspond to the oxidation of the 1,4-dihydropyridine moiety. This conclusion is further supported by other additional experimental facts, mainly derived from the GC–MS characterization.

Concluding, the electrochemical oxidation of these type of 1,4-dihydropyridines in aprotic medium is deeply affected by changes in the acid–base equilibrium of the oxidizable groups. In the case of 4-phenyl-DHP derivative which exclusively contains one N–H ionizable group, the oxidation process involves the anion ( $\text{R}-\text{N}^-$ ) and the respective conjugated acid ( $\text{R}-\text{NH}$ ), giving at least two oxidation signals, depending on the electrolytic media. In contrast, for the hydroxyphenyl-substituted 1,4-dihydropyridines, the electrochemical oxidation could involve signals corresponding to the unionized and ionized species of both oxidizable groups, that is, the 1,4-dihydropyridine moiety and the hydroxyl group substituting the aromatic ring of the 4-position.

### 2.3. UV–visible spectrophotometry

UV–vis spectra for each compound were recorded between 200 and 700 nm. In Table 1, UV–visible bands

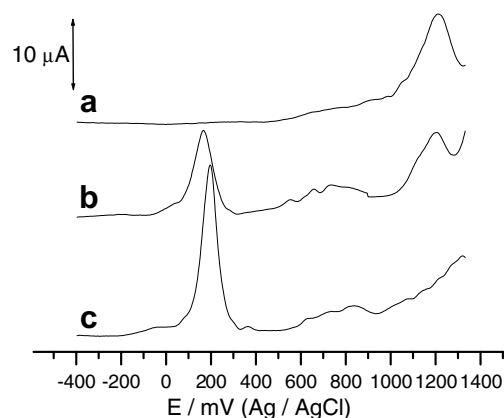


**Figure 3.** DP voltammograms of: (a) 1 mM phenol solution in dimethylsulfoxide. (b) Solution (A) +2.0 mM TBA-OH. (c) Solution (D) +4.0 mM TBA-OH.

and molar absorptivities for 1,4-dihydropyridines in dimethylsulfoxide and in the presence of TBA-OH are presented. As can be seen from Table 1, all compounds exhibited a common maximum at 358 nm. The hydroxyphenyl-substituted 1,4-DHP derivatives exhibited additional bands in the zone of 278–283 nm. Figure 4a shows a typical UV–vis spectrum for 4-(4-hydroxyphenyl)-DHP derivative. Addition of 250  $\mu\text{M}$  TBA-OH produces a drastic bathochromic effect, shifting the band at 358 nm toward 447 nm and the band at 278 nm to 323 nm as shown in Figure 4b. The effect is due to anion formation in the basic medium. The band at 447 nm gradually disappeared after the addition of 250  $\mu\text{M}$   $\text{HClO}_4$  solution, turning these solutions to its original colors (Fig. 4c). These results can be explained on the basis of the acid–base equilibrium involving the  $-\text{NH}$  group. In the presence of a TBA-OH solution, predominantly the equilibrium is displaced toward the anionic form ( $\text{R}-\text{N}^-$ ), which absorbs at 447 nm. The negative charge can be de-localized over the system up to the ester groups in 3- and 5-position, thus explaining the appearance of colored solutions in this medium. Clearly, molar absorptivity values corresponding to the 1,4-dihydropyridine anions are significantly higher than those of the unionized compounds (Table 1).

#### 2.4. Controlled-potential electrolysis (CPE) experiments

In the present paper, we have used exhaustive controlled-potential electrolysis on reticulated carbon electrode to oxidize the 1,4-DHP solutions and to generate the radical intermediates (dihydropyridyl radical), which were trapped by PBN. However, the generation of these unstable species can also be obtained by using chemical, photochemical or enzymatic procedures.<sup>30</sup> On the other hand, the electrolyzed solutions were analyzed by GC–MS and ESR techniques in order to identify the oxidation product(s) and the intermediates, respectively.

**2.4.1. GC–MS studies.** In Table 2, the GC–MS data of studied compounds are reported. The three synthesized 1,4-dihydropyridines follow a general fragmentation pathway which corresponds to the cleavage and complete loss of the substituent in 4-position, to give a common mass fragment with  $m/z$  of 252. Concerning with the analyses of electrolyzed 1,4-DHP solutions,

**Table 1.** UV–visible absorption bands and molar absorptivity of 1,4-DHP derivatives and their corresponding anions

Compounds	Molar absorptivity/(M cm) <sup>-1</sup>			
	$\lambda = 278\text{--}283$ nm <sup>a</sup>	$\lambda = 358$ nm <sup>a</sup>	$\lambda = 323$ nm <sup>b</sup>	$\lambda = 447$ nm <sup>b</sup>
4-Phenyl-DHP	—	6299	—	10,900
4-(3-Hydroxyphenyl)-DHP (283 nm)	2322	6451	2341	11,733
4-(4-Hydroxyphenyl)-DHP (278 nm)	5225	8633	5416	15,870

<sup>a</sup> UV–visible bands obtained in dimethylsulfoxide.

<sup>b</sup> UV–visible bands obtained in dimethylsulfoxide + 250  $\mu\text{M}$  TBA-OH corresponding to the formation of the anion.

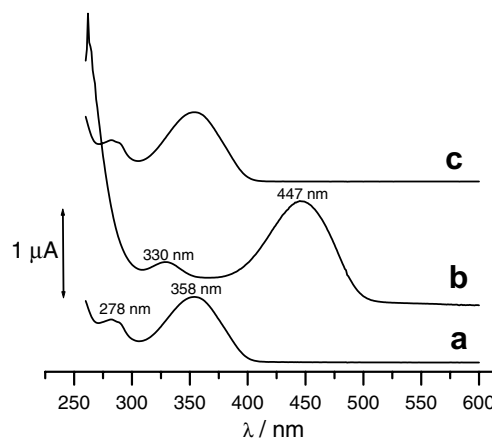


**Figure 4.** UV–vis spectra of: (a) 1 mM 4-(4-hydroxyphenyl)-DHP solution in dimethylsulfoxide. (b) Solution (A) +7 mM TBA-OH. (c) Solution (B) +250  $\mu\text{M}$   $\text{HClO}_4$ .

they were derivatized with *N*-methyl-*N*-(trimethylsilyl)-trifluoroacetamide (MSTFA) previous to the injection into the chromatograph to improve their chromatographic characteristics. The results obtained after 90 min of CPE are illustrated in Figure 5 for 4-(3-hydroxyphenyl)-DHP. A typical mass spectrum of this compound is displayed in this Figure 5. Three most abundant mass fragments containing the pyridine nucleus were found. These fragments had  $m/z$  415,  $m/z$  354, and  $m/z$  326, respectively. Consistently, the most abundant fragment was  $m/z$  415, which corresponds to the oxidation of the 1,4-dihydropyridine moiety to give rise to the pyridine derivative. The mass fragment with  $m/z$  354 corresponds to the simultaneous cleavage of an ethoxy group and a methyl group of the TMS moiety. The third most abundant fragment was the  $m/z$  326, which corresponded to the complete loss of TMS group. Also, the % formed pyridine during the electrolysis was quantitatively assayed (Table 2), no significant differences were found between the compounds, in all the cases the percentages were lower than 50%.

Summarizing, the results obtained by the GC–MS technique permit us the identification of the pyridine derivatives as the final products of the electrolytic oxidation of 1,4-dihydropyridines.

**2.4.2. ESR.** To identify the intermediates produced in the time-course of the electrolysis of 1,4-dihydropyridine derivatives, spin trapping studies were conducted. The experimental ESR spectra show a triplet, due to the nitrogen, and their splitting into a doublet due to the presence of the adjacent hydrogen. The corresponding  $a_{\text{N}}$  values were: 13.2 G, 12.1 G, and 12.1 G for 4-phenyl-DHP, 4-(3-hydroxyphenyl)-DHP, and 4-(4-hydroxyphenyl)-DHP, respectively. On the other hand,  $a_{\text{H}}$  splitting values for the same compounds were: 3.5 G, 2.8 G, and 2.5 G, respectively. In Figure 6 the experimental ESR spectra corresponding to the three derivatives are shown. Simulated spectra (data not shown) were in good agreement with the experimental one.

**Table 2.** GC–MS data obtained from parent and oxidized 1,4-DHP derivatives

Derivative	Parent 1,4-DHP		Oxidized 1,4-DHP		% Pyridine <sup>a</sup>
	M+	Pb	M+	Pb	
4-Phenyl-DHP	331	252	329	327	38.5
4-(3-Hydroxyphenyl)-DHP	417	252	415	415	43.3
4-(4-Hydroxyphenyl)-DHP	417	252	415	415	42.1

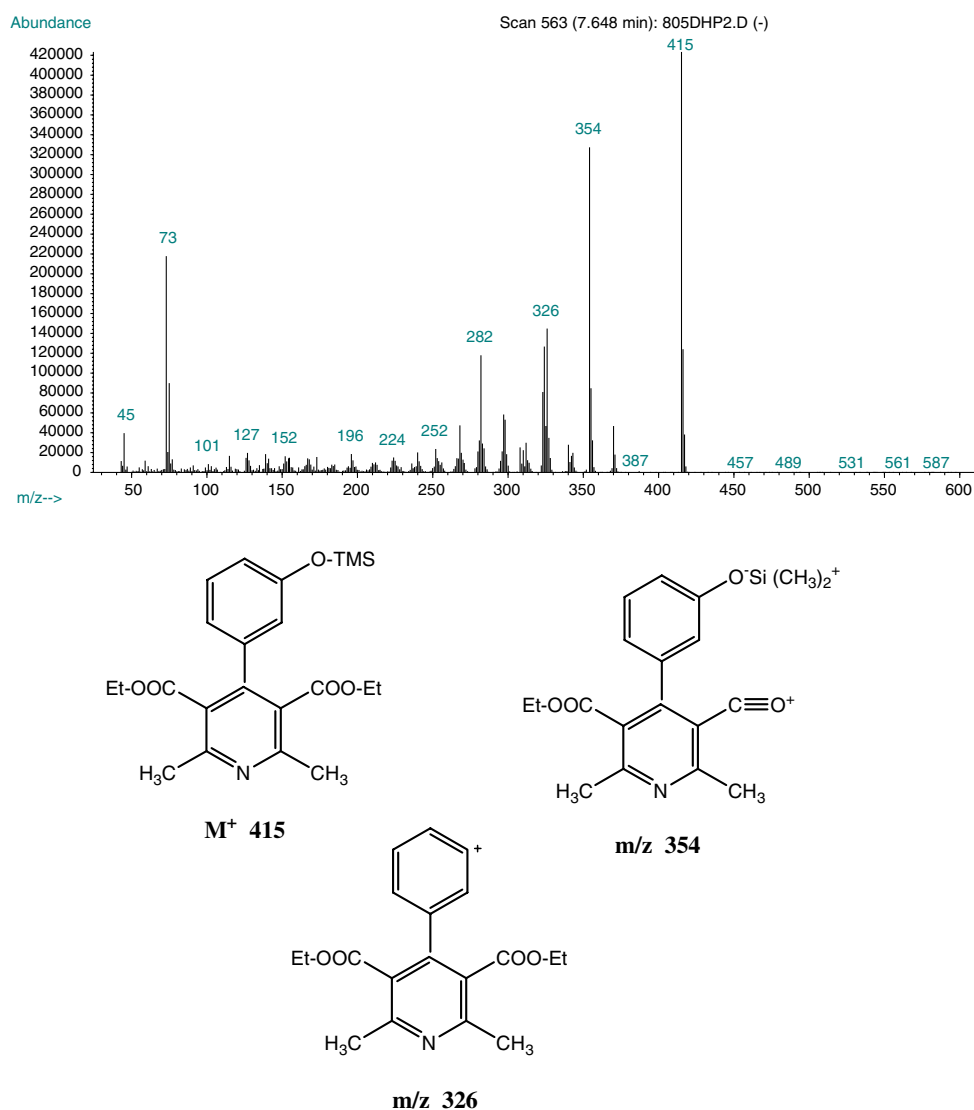
M<sup>+</sup>, molecular ion.

Pb, peak base.

<sup>a</sup> Percentage of pyridine after 90 min electrolysis.

The above splitting constants for the spin adducts are consistent with the fact that *N-tert*-butylamine- $\alpha$ -phenylnitron (PBN) interacted with carbon-centered radicals as reported for 1,4-DHP derivatives<sup>31</sup> and for other structurally related compounds.<sup>32</sup> It is a well-known fact that the radical adducts may be carbon-centered or nitrogen-centered depending strongly on the nature of spin trap used. We are currently working with PBN, a spin trap having

the advantage of forming very stable C-centered radical adducts because of its stability. Also, other spin-trapping have been used in electrochemistry like aryl nitroso compounds.<sup>33</sup> These agents are light sensitive implying some difficulties in certain experimental conditions, but nitroxide formation results in a trapped radical bound to the nitrogen atom, thus giving extra ESR information which is not obtained by using PBN.<sup>34</sup>

**Figure 5.** Mass fragmentation spectrum corresponding to the oxidized 4-(3-hydroxyphenyl)-DHP after 90 min of electrolysis.



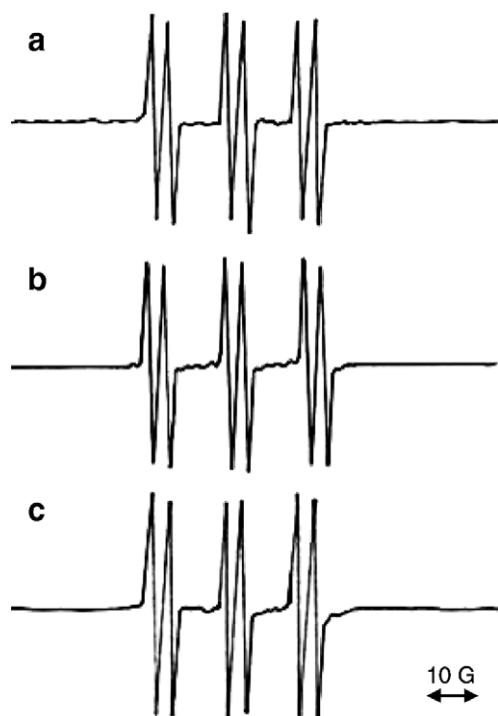


**Figure 6.** ESR spectra of: (a) 4-phenyl-1,4-DHP. (b) 4-(3-Hydroxyphenyl)-DHP. (c) 4-(4-Hydroxyphenyl)-DHP.

### 2.5. Reactivity with ABAP-derived alkylperoxyl radicals

Considering that peroxy radicals play an important role in chemistry and biology,<sup>35</sup> and that they are involved in many radical chain reactions, for example lipid peroxidation and protein damage<sup>36</sup>, we decide to prove the reactivity of the synthesized 1,4-DHPs with ABAP-derived alkylperoxyl radicals in aqueous medium, pH 7.4. For these studies we used UV-vis spectroscopy and GC-MS techniques.

For the spectroscopic studies, the original UV absorption bands between  $\lambda = 356\text{--}360\text{ nm}$  were followed to evaluate reactivity. The results revealed that after the addition of 1,4-DHP derivatives to an aqueous mixture containing alkylperoxyl radicals, the absorption bands decreased along time (Fig. 7a), parallel with the appearance of a new band near to 280 nm (Fig. 7b). This latter signal corresponds to the oxidized derivative, that is, the pyridine derivative, which agrees with previous observations.<sup>37</sup> The rate of reaction exhibited a linear dependence on concentration in the range of 20–120  $\mu\text{M}$  concentration of 1,4-DHP. To compare the reactivity, kinetic rate constants of tested 1,4-DHP derivatives and kinetic rate constants of the corresponding reference compounds (NADH and Nisoldipine) were used (Table 3). Clearly, the synthesized 1,4-DHP derivatives were significantly more reactive than nisoldipine, a commercial 1,4-DHP used in therapeutics. In conclusion, all the synthesized compounds were at least 2.4 times more reactive than this well-known antioxidant drug (Table 3). However, the most reactive compound was NADH, an endogenous compound structurally related with 1,4-dihydropyridines. At the end of the experiments, samples

were derivatized with MSTFA and injected into the chromatograph. Results of these analyses confirm that after the reaction between the alkylperoxyl radicals and the tested 1,4-dihydropyridines, these latter derivatives were oxidized to pyridines. The mass fragmentation pathways did not differ from that of electrolysis, that is, the fragments contained the pyridine nucleus, being the most abundant  $m/z$  415,  $m/z$  354, and  $m/z$  326.

### 3. Concluding remarks

- The electrochemical oxidation of C4- hydroxyphenyl-substituted 1,4-DHPs in DMSO occurs involving 2-protons and 2-electrons with formation of a dihydropyridyl radical intermediate and the pyridine derivative as the final product of the oxidation. No significant effects of the C4- hydroxyl group on the oxidation of the 1,4-dihydropyridine moiety were found.
- A direct quenching of ABAP-derived alkylperoxyl radicals by three newly synthesized 1,4-DHP derivatives was found.
- The pyridine derivative was detected and quantitatively determined as a final product of the reaction between 1,4-DHP and ABAP-derived alkylperoxyl radicals.
- Our results strongly support the assumption that the reaction between the synthesized 1,4-DHP derivatives with ABAP-derived alkylperoxyl radicals involves an electron transfer reaction, which is documented by the presence of pyridine as product of reaction.

### 4. Experimental

#### 4.1. Chemicals

All solvents were of high-pressure liquid chromatography (HPLC) grade and all reagents were of analytical grade.

**4.1.1. Compounds.** 1,4-Dihydropyridine derivatives (Fig. 8) were synthesized in our laboratory according to previous works.<sup>38,39</sup> The general procedure is as follows: a mixture of 0.016 mol of the respective aldehyde (benzaldehyde, 3-hydroxybenzaldehyde, and 4-hydroxybenzaldehyde) and 3-ethyl-aminocrotonate (4.2 mL, 0.033 mol) is heated in an Erlenmeyer flask in a water bath until complete dissolution of the aldehyde. After addition of anhydrous acetic acid (15 mL), the mixture is further heated for 1 h. Temperature of the mixture must not exceed 60 °C, to avoid sub-product formation. The orange, viscous solution formed is filtered off and left until room temperature is attained. Water is carefully added (one drop at a time) until cloudiness is obtained, this is necessary to further precipitate the 1,4-dihydropyridine. The solution is warmed again to obtain a clear solution and left overnight thus permitting the slow crystallization of the derivative.

**4.1.2. 2,6-Dimethyl-3,5-diethoxycarbonyl-4-phenyl-1,4-dihydropyridine [4-phenyl-DHP].** Yield: 92%. Mp: 150–153 °C. <sup>1</sup>H NMR (300 MHz, DMSO  $\delta_6$ ):  $\delta_{\text{max}}$  1,16 (t,

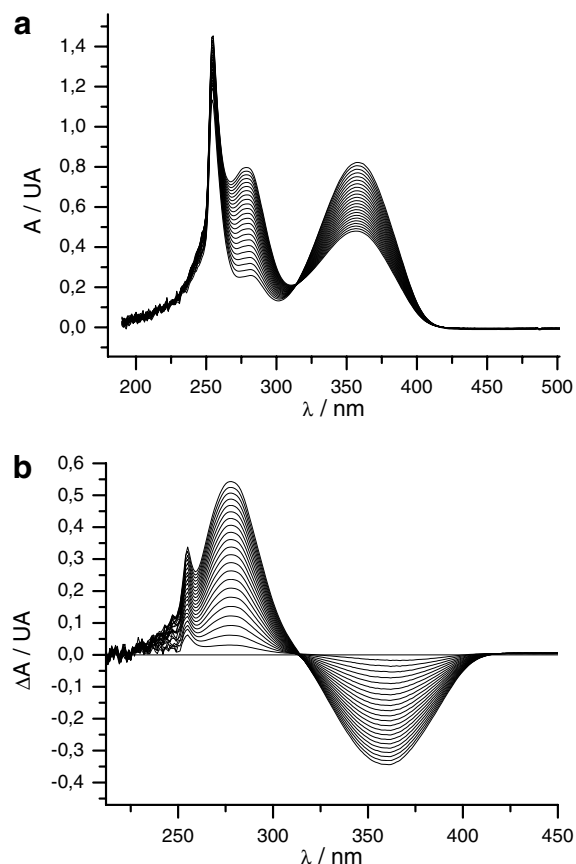


**Figure 7.** (a) UV-vis spectra corresponding to reaction between 100  $\mu\text{M}$  4-(3-hydroxyphenyl)-DHP solution and a 20 mM ABAP-derived alkylperoxyl radical solution in 0.04 M Britton-Robinson buffer /DMF 70/30 at pH 7.4. Total time: 240 min. (b) Differential UV-visible spectra.

**Table 3.** Comparison of the reactivity of C4-substituted 1,4-DHP derivatives towards alkylperoxyl ABAP-derived radicals

Derivative	$k^a \cdot 10^{-5} \text{s}^{-1}$	$k/\text{Nisoldipine}^b$	$R/\text{NADH}^c$
NADH	$3.80 \pm 0.01$	18.1	1.00
4-Phenyl-DHP	$0.51 \pm 0.02$	2.4	0.13
4-(3-Hydroxyphenyl)-DHP	$0.64 \pm 0.01$	3.0	0.17
4-(4-Hydroxyphenyl)-DHP	$0.60 \pm 0.02$	2.9	0.16
Nisoldipine	$0.21 \pm 0.01$	1.0	0.06

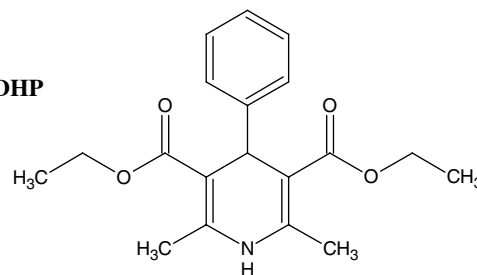
<sup>a</sup> Kinetic rate constants for the reactivity of the derivatives in the presence of alkylperoxyl radicals. Values correspond to the average of five independent experiments.

<sup>b</sup> Ratio between kinetic rate constants of the tested 1,4-DHP derivatives/kinetic rate constant of nisoldipine for the reaction with alkylperoxyl radicals.

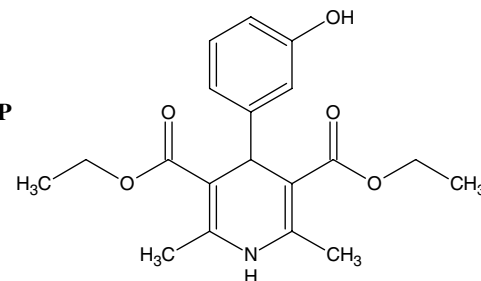
<sup>c</sup> Ratio between the kinetic rate constants of the tested 1,4-DHP derivatives/kinetic rate constant of NADH for the reaction with alkylperoxyl radicals.

6H,  $2 \times -\text{CH}_2-\text{CH}_3$ ); 2.26 (s, 6H,  $2 \times -\text{CH}_3$ ); 3.98 (q, 4H,  $2 \times -\text{O}-\text{CH}_2-\text{CH}_3$ ); 4.88 (s, 1H, Ar-CH<); 7.18 (m, 3H,  $J = 6.975 \text{ Hz}$ ,  $3 \times \text{Ar-H}$ ); 7.22 (d, 2H,  $J = 8.14 \text{ Hz}$ ,  $2 \times \text{Ar-H}$ ); 8.80 (s, 1H, N-H).  $^{13}\text{C}$  NMR (75 MHz, DMSO  $\delta_6$ ): 10.51; 9.26; 9.07; 7.88; 7.78; 6.18; 2.09; 2.05; 2.04; 1.97; 0.63.

**4-phenyl-DHP**



**3-OH-DHP**



**4-OH-DHP**

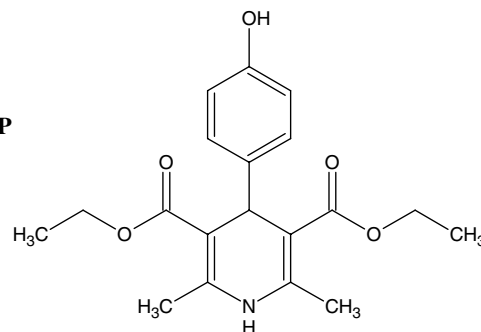


**Figure 8.** Chemical structures of the synthesized compounds.

**4.1.3. 2,6-Dimethyl-3,5-diethoxycarbonyl-4-(3-dihydroxyphenyl)-1,4-dihydropyridine [4-(3-hydroxyphenyl)-DHP].** Yield: 85%. Mp: 188–191 °C. IR (KBr):  $\delta_{\text{max}}$  3351.1, 1649.8, 1594.5, 1473.3, 1367.6, 1216.8, 1127.6, 1018.4.  $^1\text{H}$ NMR (300 MHz, acetone- $d_6$ ): 1.2 (t,  $J = 7.0$ , 6H,  $-\text{CH}_3$ ); 2.3 (s, 6H,  $-\text{CH}_3$ ); 2.9 (s, 1H, C-H); 4.1 (q,  $J = 7.0$ , 4H,  $-\text{CH}_2$ ); 5.0 (s, 1H, -OH); 6.9 (m, 4H, aromatic); 7.8 (s, 1H, N-H).  $^{13}\text{C}$ RMN (75 MHz, acetone- $d_6$ ): 13.8(2); 17.9(2); 29.0; 38.6; 58.9(2); 103.3(2); 114.4(2); 115.0; 119.1; 130.5; 144.3; 165.3; 205.5.

**4.1.4. 2,6-Dimethyl-3,5-diethoxycarbonyl-4-(4-hydroxyphenyl)-1,4-dihydropyridine [4-(4-hydroxyphenyl)-DHP].** Yield: 70%. Mp: 232 - 235 °C. IR (KBr):  $\delta_{\text{max}}$  3354.1, 1655.8, 1591.7, 1478.5, 1367.1, 1220.3, 1122.4, 1019.7.  $^1\text{H}$ NMR (300 MHz, acetone- $d_6$ ): 1.2 (t,  $J = 7.0$ , 6H,  $-\text{CH}_3$ ); 2.3 (s, 6H,  $-\text{CH}_3$ ); 2.9 (s, 1H, C-H); 4.1 (q,  $J = 7.0$ , 4H,  $-\text{CH}_2$ ); 5.0 (s, 1H, -OH); 6.6 (d,  $J = 8.0$ , 2H, aromatic); 6.8 (d,  $J = 8.0$ , 2H, aromatic); 7.8 (s, 1H, N-H).  $^{13}\text{C}$ RMN (75 MHz, acetone- $d_6$ ): 13.6(2); 18.3(2); 30.0; 37.9; 59.3(2); 107.5(2); 113.2(2); 118.0; 119.3; 132.7; 141.2; 161.4(2); 207.3.

NMR spectroscopy: The NMR spectra were recorded on a Bruker spectrometer Advance DRX 300.

FT-IR: The IR spectra were recorded on a Bruker spectrometer IFS 55 Equinox.

**4.1.5. Aprotic medium.** Dimethylsulfoxide (DMSO) + 0.1 M tetrabutylammonium hexafluorophosphate (TBAHFP) was used for the voltammetric experiments.

## 4.2. Voltammetry

Differential Pulse (DPV), cyclic (CV), and dynamic voltammetry were performed with a BAS CV 100 assembly. A glassy carbon stationary electrode as working electrode for DPV and CV experiments was used. For dynamic experiments a glassy carbon rotating disk electrode was also employed. A platinum wire was used as a counter electrode and all potentials were measured against an Ag/AgCl electrode.

**4.2.1. Coulometric analysis.** These studies were performed on exhaustive electrolysis at constant electrode potential at +1180 mV versus Ag/AgCl for the derivatives on a glassy carbon coil electrode. The measurements were carried out on a BAS CV 100 analyzer using a two-compartment electrolytic cell and the derivatives were dissolved in DMSO + 0.1 M TBAHFP. The net charge was calculated by correction for the estimated background current.

**4.2.2. Controlled-potential electrolysis (CPE).** CPE was carried out on a reticulated carbon electrode in anhydrous DMSO + 0.1 M TBAHFP at +1180 mV for all 1,4-DHPs. A three-electrode circuit with an Ag/AgCl electrode was used as reference and a platinum wire as a counter electrode. A BAS-CV 100 assembly was used to electrolyze the different derivatives.

## 4.3. UV-visible spectroscopy

The UV-visible characterization of the compounds and the progress of the reactivity with free radicals were followed by using an Agilent Spectrophotometer UV-visible with diode array. Spectra were recorded in the 220–700 nm range at different intervals. Acquisition and data treatment were carried out with a HP UV-visible win system.

## 4.4. ESR

Spectra were recorded in situ on a Bruker spectrometer ECS 106 with 100 kHz field modulation in X band (9.78 GHz) at room temperature. The hyperfine splitting constants were estimated to be accurate within 0.05 G. The electrolysis was performed in the ESR cell using an appropriate platinum mesh electrode according to the same conditions as described above. The concentration of the 1,4-DHP derivatives was 1.0 mM. *N*-tert-butylamine- $\alpha$ -phenylnitron (PBN) was used as spin trap at a concentration of 100 mM.

## 4.5. GC-MS

A Gas Chromatograph/Mass Selective 6890/5973 Detector (Hewlett-Packard, Palo Alto, California, USA) and

Hewlett Packard 7673 Auto sampler were used for the analyses. Hewlett Packard Data System was used to control the instrumentation and data processing. The *m/z* monitored range was 43–600, 1 scan/s scan rate; normal energy electron, 70 eV.

**4.5.1. Column chromatography.** Hewlett-Packard Ultra-1 column, 25 m  $\times$  0.2 mm id  $\times$  0.11  $\mu$ m film thickness (Little Falls, Wilmington, Delaware, USA).

Chromatographic conditions: Detector temperature, 300 °C; Injector temperature, 250 °C; split ratio, 1:10; pressure, 25 psi; purge flow, 50 mL min<sup>-1</sup>; purge time, 0.5 min.

Temperature program: oven temperature was programmed from 120 to 310 °C (hold for 3 min) at 17 °C min<sup>-1</sup>; run time, 14.18 min. Helium was used as carrier gas, inlet pressure, 35 kPa.

**4.5.2. Derivatization procedure.** After controlled-potential electrolysis experiments or the reactivity reactions with ABAP-derived alkylperoxyl radicals, the samples were diluted with ethanol to obtain final concentrations of about 0.1 mM, evaporated to dryness under a gentle helium flux, and derivatized with 100  $\mu$ L MSTFA (*N*-methyl-*N*-(trimethylsilyl)-trifluoroacetamide, Sigma-Aldrich) by heating at 75 °C for 30 min and then, the derivatized extracts were injected into the chromatograph.

## 4.6. Reactivity toward alkylperoxyl ABAP-derived radicals

ABAP (2,2'-azobis (2-amidinopropane) dihydrochloride, Aldrich Chemical Company) was used as radical generator for the radicals. Different series of 20 mM ABAP solutions in 0.04 M Britton-Robinson buffer/DMF 70/30, pH 7.4, at a constant ionic strength of 0.1 M adjusted with KCl were incubated with 100  $\mu$ M solutions of each 1,4-DHP or NADH at 37 °C for 120 min with constant bubbling of oxygen. The rate of alkylperoxyl radical formation from this initiator is constant at a given temperature.<sup>40</sup> But, the rate of alkylperoxyl radical formation from ABAP will not be constant as it depends upon the concentration of ABAP (rate =  $k$  [ABAP]). It appears that, over 120 min at 37 °C, only a small amount of the ABAP will decay, therefore the rate may be considered constant at 37 °C. In neutral aqueous solutions, the half-life of ABAP is about 175 h, and the generation rate of radicals is constant for the first few hours.<sup>41</sup> Control solutions containing either 1,4-DHP or NADH solutions were run in the same conditions as the above mixtures. Time-course of the reactivity of synthesized 1,4-DHP derivatives with the generated alkylperoxyl radicals was followed by UV/visible spectroscopy and GC-MS technique.

For the determination of kinetic rate constants for the reactivity between the 1,4-DHP derivatives and alkylperoxyl radicals, a pseudo first-order kinetic condition was used.



$$V = K \times [1,4\text{-DHP}] \times [\text{ROO}\cdot]$$

In our experimental conditions,  $[1,4\text{-DHP}] \lll [\text{ROO}\cdot]$ , then

$$V = K' \times [1,4\text{-DHP}]$$

The reactivity toward alkylperoxyl radicals was expressed in comparison either with NADH or commercial 1,4-DHPs using the following ratio:

*Slope DHP tested/slope NADH or commercial derivative*, where the slope refers to the respective concentration–time plots in presence of free radicals. Control solutions (in the absence of ABAP-derived radicals) revealed no changes either in their original UV/visible absorption bands or GC–MS mass fragmentation. Also, a possible photodecomposition of 1,4-dihydropyridines was assessed, but in the time-scale of the experiments this was negligible.

### Acknowledgments

This work was supported by Project FONDECYT 1050761.

### References and notes

- Triggle, David J. *Drug Dev. Res.* **2003**, *58*, 5–17.
- Liang, J.-Ch.; Yeh, J.-L.; Wang, Ch.-S.; Liou, S.-F.; Tsai, Ch.-H.; Chen, I.-J. *Bioorg. Med. Chem.* **2002**, *10*, 719–730.
- Budriesi, R.; Bisi, A.; Ioan, P.; Rampa, A.; Gobbi, S.; Belluti, F.; Piazzzi, L.; Valenti, P.; Chiarini, A. *Bioorg. Med. Chem.* **2005**, *13*, 3423–3430.
- Varma, R. S.; Kumar, D. *Tetrahedron Lett.* **1999**, *40*, 21–24.
- Zhu, X.-Q.; Zhao, B.-J.; Cheng, J.-P. *J. Org. Chem.* **2000**, *65*, 8158–8163.
- Zhu, X.-Q.; Liu, Y. C.; Cheng, J.-P. *J. Org. Chem.* **1999**, *64*, 8980–8981.
- Valenti, P.; Rampa, A.; Budriesi, R.; Bisi, A.; Chiarini, A. *Bioorg. Med. Chem.* **1998**, *6*, 803–810.
- Peri, R.; Padmanabhan, S.; Rutledge, A.; Singh, S.; Triggle, D. J. *J. Med. Chem.* **2000**, *43*, 2906–2914.
- Bocker, R. H.; Guengerich, P. J. *J. Med. Chem.* **1986**, *29*, 1596–1603.
- Itoh, T.; Nagata, K.; Matsuya, Y.; Miyazaki, M.; Ohsawa, A. *J. Org. Chem.* **1997**, *62*, 3582–3585.
- Turovska, B.; Stradins, J.; Turovskis, I.; Plotniece, A.; Shmidlers, A.; Duburs, G. *Chem. Heterocyc. Comp.* **2004**, *40*, 753–758.
- Baumane, L.; Krauze, A.; Belyakov, S.; Sile, L.; Chernova, L.; Griga, M.; Duburs, G.; Stradins, J. *Chem. Heterocyc. Comp.* **2005**, *41*, 362–373.
- García Rosales, A.; Ruiz Montoya, M.; Marín Galvín, R.; Rodríguez Mellado, J. M. *Electroanalysis* **1999**, *11*, 32–36.
- Stradins, J.; Ogle, J.; Kadysh, V.; Baumane, L.; Gavars, R.; Duburs, G. *J. Electroanal. Chem.* **1987**, *226*, 103–116.
- Ogle, J.; Stradins, J.; Baumane, L. *Electrochim. Acta* **1994**, *39*, 73–79.
- El Jemal, A.; Viré, J. C.; Patriarche, G. J.; Nieto Palmeiro, O. *Electroanalysis* **1992**, *4*, 57–64.
- Ludvik, J.; Turecek, F.; Volke, J. *J. Electroanal. Chem.* **1985**, *188*, 105–109.
- J Nuñez-Vergara, L.; Sturm JC, J. C.; Alvarez-Lueje, A.; Olea-Azar, C.; Sunkel, C.; Squella, J. A. *J. Electrochem. Soc.* **1999**, *146*, 1478–1485.
- Nuñez-Vergara, L. J.; Ortiz, M. E.; Bollo, S.; Squella, J. A. *Chem. Biol. Interact.* **1997**, *106*, 1–14.
- López-Alarcón, C.; Squella, J. A.; Miranda-Wilson, D.; Nuñez-Vergara, L. J. *Electroanalysis* **2004**, *16*, 539–546.
- López-Alarcón, C.; Nuñez-Vergara, L. J.; Squella, J. A. *Electrochim. Acta* **2003**, *48*, 2505–2516.
- Nuñez-Vergara, L. J.; López-Alarcón, C.; Navarrete-Encina, P. A.; Atria, A. M.; Camargo, C.; Squella, J. A. *Free Radic. Res.* **2003**, *37*, 109–120.
- Sobal, G.; Menzel, E. J.; Sinzinger, H. *Biochem. Pharmacol.* **2001**, *61*, 373–379.
- Berkels, R.; Breitenbach, Th.; Bartels, H.; Taubert, D.; Rosenkranz, A.; Klaus, W.; Roesen, R. *Vas. Pharmacol.* **2005**, *42*, 145–152.
- Cominacini, L.; Pasini, A. F.; Garbin, U.; Pastorino, A. M.; Davoli, A.; Nava, C.; Campagnola, M.; Rossato, P.; Lo Cascio, V. *Biochem. Biophys. Res. Commun.* **2003**, *302*, 679–684.
- Yañez, C.; López-Alarcón, C.; Camargo, C.; Valenzuela, V.; Squella, J. A.; Nuñez-Vergara, L. J. *Bioorg. Med. Chem.* **2004**, *12*, 2459–2468.
- Tong Mak, I.; Zhang, J.; Weglicki, W. B. *Pharmacol. Res.* **2002**, *45*, 27–33.
- van Amsterdam, F. T. M.; Roveri, A.; Maiorino, M.; Ratti, E.; Ursini, F. *Free Radic. Biol. Med.* **1997**, *12*, 183–187.
- Adams, R. N. In *Electrochemistry at Solid Electrodes*; Bard, A. J., Ed.; Marcel Dekker: New York, 1969; p 154.
- Marchesi, E.; Rota, C.; Fann, Y. C.; Chignell, C. F.; Mason, R. P. *Free Radic. Biol. Med.* **1999**, *26*, 148–161.
- Rota, C.; Fann, Y. C.; Mason, R. P. *J. Biol. Chem.* **1999**, *274*, 28161–28168.
- Klima, J.; Ludvik, J.; Volke, J.; Krikava, M.; Skala, V.; Kuthan, J. *J. Electroanal. Chem.* **1984**, *161*, 205–211.
- Srividya, N.; Ramamurthy, P.; Shanmugasundaram, P.; Ramakrishnan, V. T. *J. Org. Chem.* **1996**, *61*, 5083–5089.
- Klíma, J.; Volke, J.; Urban, J. *Electrochim. Acta* **1991**, *36*, 73–77.
- Frei, B.; Stocker, R.; Ames, B. N. *Proc. Natl. Acad. Sci. U.S.A.* **1988**, *85*, 9748–9752.
- Marnett, L. J. *Carcinogenesis* **1987**, *8*, 1365–1373.
- Labudzinska, A.; Gorczynska, K. *J. Mol. Struct.* **1995**, *349*, 469–472.
- Lavilla, R. *J. Chem. Soc., Perkin. Trans. 1* **2002**, 1141–1156.
- Navarrete-Encina, P. A.; Conde, B.; Carbajo, J.; Camargo, C.; Squella J. A.; Nuñez-Vergara, Luis J. *Synth. Comm.*, in press.
- Halliwell, B.; Gutteridge, J. M. C. *Free Radicals in Biology and Medicine*; Oxford: University Press: New York, 2000, pp 69–70.
- Niki, E. *Methods Enzymol.* **1990**, *186*, 100.